Microstructure Investigation and Mechanical Properties of Resistance Upset Butt Welded Ti-6Al-4V Alloy

Mahmood Sharifitabar*
Department of Materials Engineering,
University of Sistan and Baluchestan, Zahedan, Iran
E-mail: msharifitabar@eng.usb.ac.ir
*Corresponding author

Received: 27 January 2020, Revised: 15 February 2020, Accepted: 20 February 2020

Abstract: In the present study, resistance upset butt welding was used as a solid-state process for joining Ti-6Al-4V alloy. Results showed that melting and subsequent solidification of the alloy at the joint interface promoted the development of a cast microstructure along with some pores. However, by applying the constant upset pressure of 1.62 MPa, the pore volume fraction decreased considerably with decreasing the welding current from 110 A/mm^2 to 55 A/mm^2. Hardness test results showed that the weld interface and the base material had the highest (352 HV) and the lowest (318 HV) values, respectively. The microstructure of the interface consisted of ά martensite and Widmanstätten laths. The tensile strength of the joints varied between 550 and 883 MPa depending on the welding parameters used. In the optimum condition, the maximum strength of the joint was about 94% of the base metal strength. Fractography of samples confirmed that the formation of pores deteriorated the strength of the joints.

Keywords: Fractography, Microstructure, Solid-State Welding, Ti-6Al-4V Alloy, Weld Defect

Reference: Mahmood Sharifitabar, "Microstructure Investigation and Mechanical Properties of Resistance Upset Butt Welded Ti-6Al-4V Alloy", Int J of Advanced Design and Manufacturing Technology, Vol. 13/No. 3, 2020, pp. 91–97. DOI: 10.30495/admt.2020.1891939.1170.

Biographical notes: Mahmood Sharifitabar received his MSc degree in Metallurgical and Materials Engineering, Welding Branch from the University of Tehran in 2009 and his PhD degree in Materials Engineering from the Ferdowsi University of Mashhad in 2015. He is currently Assistant Professor at the Department of Materials Engineering, Faculty of Engineering, University of Sistan and Baluchestan, Zahedan, Iran. His current research interest includes Welding and Cladding, Additive Manufacturing of Metals and Alloys, and Combustion Synthesis of Materials.

1 INTRODUCTION

As one of the most common titanium alloys, Ti-6Al-4V is widely used in medical, aerospace, chemical and marine industries due to the high strength to weight ratio, good corrosion, and oxidation resistance and biocompatibility [1-2]. Welding of this alloy with common fusion welding processes accompanies with some problems because molten titanium rigorously reacts with oxygen, hydrogen and nitrogen during welding which in turn decreases the ductility of the alloy, severely [2]. Moreover, the formation of brittle cast structure and non-equilibrium phases, grain growth in the heat-affected zone (HAZ) and the development of pores are other related welding difficulties [1-3]. Many of these problems can be overcome using solid-state welding processes like friction welding [4], friction stir welding [5], explosive welding [6], and resistance upset welding (RUW).

RUW is a solid-state welding process in which the joining surfaces are kept in contact with each other using a constant pressure (heating pressure). Then, the electrical current is passed through the contact area. Passage of electrical current produces high heat in this region. Simultaneous application of pressure and current will cause the components to join to each other [7-13]. The general configuration of parts and equipment used in RUW is shown in “Fig. 1” [9], [13]. Welding time which is the passing time of electrical current through the parts, welding current and upset pressure are the main parameters which can influence the quality of the joints.

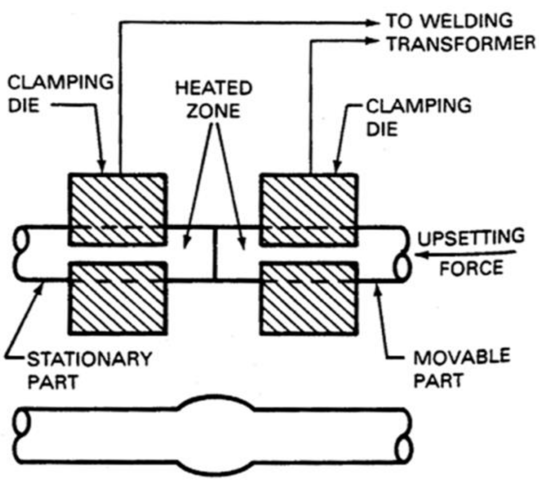

Fig. 1 Schematic illustration of resistance upset butt welding process [9].

Up to now, RUW has been used for welding of various alloys such as carbon steel, aluminum, superalloys, stainless steels and zirconium alloy [7], [10-13]. Min et al. [14] used the RUW process for joining a special kind of steel sheet (SPCC) that is used in the automobile industry. Then, they evaluated the quality of the joints by tensile and Erichsen cup tests. Their results showed that the tensile strength of the joint was similar to the base material. Moreover, cracks did not occur in the weld metal after the Erichsen test. Kerstens and Richardson [15] simulated the heat distribution in resistance upset welding by applying different welding parameters. Their results confirmed uneven distribution of welding current along the faying surfaces which led to the formation of hot spots with cast microstructure. Hamedi et al. [9] simulated the effects of welding current and time on the tensile strength of RUW joints. Moreover, they compared the simulated results with the experimental data. It was shown that variation in the welding current had a stronger effect on strength than the welding time. Moreover, the strength of the joint increased with increasing the welding current and time; reached a maximum value and then decreased.

In a similar study Le Gloannec et al. [16] simulated RUW in the rod to tube geometry and found a good agreement between the simulated results with the experimental observations. The effects of RUW parameters on the microstructure and mechanical properties of various engineering alloys were considered by many researchers. Sharifitabar et al. [13] investigated the effect of welding parameters on microstructure and mechanical properties of 304 stainless steel welds. They showed the microstructure of the joints varied with the welding parameter. Moreover, hot spots were formed at high welding currents which deteriorated the tensile strength and fatigue properties of the joints. In another study, Sharifitabar et al. [12] considered microstructure and mechanical properties of a dissimilar joint between 304 austenitic and 420 martensitic stainless steels. They showed that a ferritic-martensitic region was developed at the interface of the joints.

Ozlati and Movahedi [17] investigated the effect of RUW parameters on the microstructure and mechanical properties of a dissimilar joint between martensitic and duplex stainless steels. Their results also confirmed that microstructure and mechanical properties of the joints were strongly influenced by welding current and optimized at a special range of parameters. All the above findings confirmed that RUW is a promising candidate for welding of engineering alloys. Moreover, welding parameters have a great influence on the microstructure and mechanical properties of the joints. Meanwhile, for each kind of alloy system, it is necessary to find the effects of RUW parameters on microstructure and mechanical properties of the joints.

Heretofore, to the best knowledge of the author, no work has been reported on the effects of RUW parameters on the microstructure and mechanical properties of Tibased alloys such as Ti-6Al-4V in the open literature. Therefore, the present study aimed to investigate the microstructure and mechanical properties of the Ti-6Al-4V welds made by resistance upset butt welding process.

2 EXPERIMENTAL PROCEDURE

Ti-6Al-4V alloy with the chemical composition of 5.8%Al, 4%V, 0.03%Fe, 0.05%Sn, 0.01%Zr, 0.02%Si and balance Ti (all in wt%) was used as starting material. This alloy was produced by vacuum arc remelting (VAR) process. Then it was hot rolled at 1123 K with a 60% reduction in area. Finally, solution treatment was performed at 1123 K for 30 minutes in order to remove rolling effects on the microstructure and its homogenization. Blocks with dimensions of 50×5×3 mm^3 were cut from the heat-treated plate. Then, their cross sections were polished using #1000 emery papers. Two blocks were placed in the upset welding machine at each step of welding. The maximum power of the welding machine was 3 KVA. This apparatus is used for welding of thin samples like saw blades with one-tenth of a millimeter to a maximum of 4 mm thickness. "Table 1" represents the welding parameters used during this research.

Table 1 Resistance upset butt welding parameters

Sample name	Current density ×10^6, A/m^2	Jaw Displacement, mm	Upset pressure, MPa
W1	110	1.95	1.62
W2	110	3.95	3.30
W3	55	1.95	1.62
W4	55	3.95	3.30

Higher jaw displacement is as a result of higher upset pressure. The selected parameters were the highest and lowest ranges of welding power and upset pressure of the welding apparatus. First, heating pressure was applied to the faying surfaces. Then the electrical current was passed through the pieces. The heat produced by Joule heating softened the material and consequently, the upset pressure led to the joining of two contacting parts. The tensile test was performed while the joint interface was in the middle of the tension specimen and the flash was machined. This test was carried out by INSTRON 4208 tensile testing machine at a displacement rate of 1 mm/min. Also, the hardness test was performed by Innova Nexus series Vickers microhardness tester by applying 200 g load for 15 seconds across the joint interface. Optical (Olympus VX51) and Scanning Electron Microscopes (SEM Cam Scan MV2300) were employed for microstructure characterization. The metallographic samples were etched with a solution containing 85%H_2O, 10%HF and 5%HCl after metallographic preparation. Finally, the fracture surface of the tensile test specimen was observed by scanning electron microscopy.

3 RESULTS AND DISCUSSION

In the upset welding process, the required heat for joining is produced by Joule heating via passing an electrical current through the interface of pieces that are in contact, together. The amount of heat produced (Q) can be calculated by the following equation [15], [18].

$$Q = RI^2t \quad (1)$$

Where, I is the current density (Ampere), R is electrical resistance (Ohms) and t is welding time. In this welding process, there are two types of resistances which play a role in heating. They are contact resistance and bulk resistance. When two samples are contacted to each other, the real contact surface area between the asperities of the surfaces is much lower than that of the theoretical contact surface area. So, at the initial state of welding, the applied current passes through these asperities. Due to their low surface area, the current density is too high and their temperature rises up, quickly. An increase in temperature softens them and they become deformed under applied pressure. The deformation of surface asperities increases the real contact surface in such a way that it gradually approaches to the theoretical one as the current passes through the abutting surfaces. Higher upset pressure causes more asperities from two surfaces to contact each other and therefore the current flow path will be more uniform. This led to the production of uniform heat along with the joint interface and a good metallurgical bond. It was previously shown that at the beginning of the joining process, more heat is produced by contact resistance, but it gradually decreases and the role of bulk resistance in heat production increases [11], [13], [18].

In the present study, for welding current, two values were selected to obtain joints with different heat input. In addition, by selecting two values for upset pressure, four joints were produced to investigate the effects of both upset pressure and welding current on the microstructure and mechanical properties of the welded samples. Figure 2 shows optical macrographs of the joint interface in W3 samples. Other samples had the same appearance, and therefore they were omitted. The heat affected zone can be distinguished from the base metal by colored lines on both sides of the interface. This discoloration around the interface shows atmospheric contamination and subsequent oxidation of this region during welding [19].

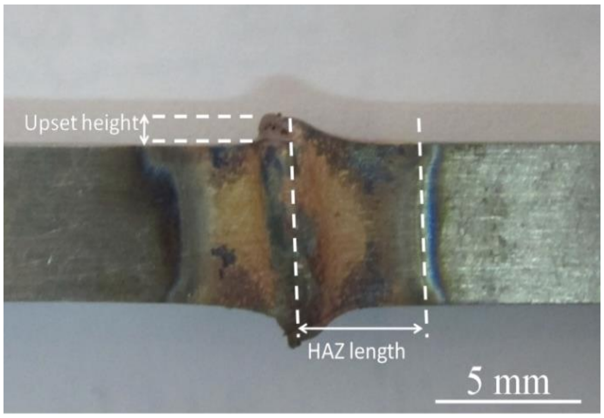

Fig. 2 Macrograph of the joint interface in W1 sample.

In solid-state welding processes like resistance upset welding, flash butt welding and friction welding, application of upset pressure causes repulsion of melt and mushy metal from the joint interface during coalescence [9]. This leads to the formation of an upset around the contact surfaces. The formation of upset is necessary for this welding technique because it removes some un-wanted phases like surface oxides and melted metal from the interface and guarantees the weld soundness. However, the development of extra upset may have detrimental effects on the weld quality. Therefore, controlling the upset height may be considered as an indirect measure of the weld quality. The height of the upset is dependent on the contacting surface roughness, welding heat input and upset pressure, considerably and usually increases with increasing the two last parameters. On the other hand, the width of the Heat-Affected Zone (HAZ) is also related to the welding heat input and upset pressure. Figure 3 shows the measured width of HAZ and upset height in different welded samples.

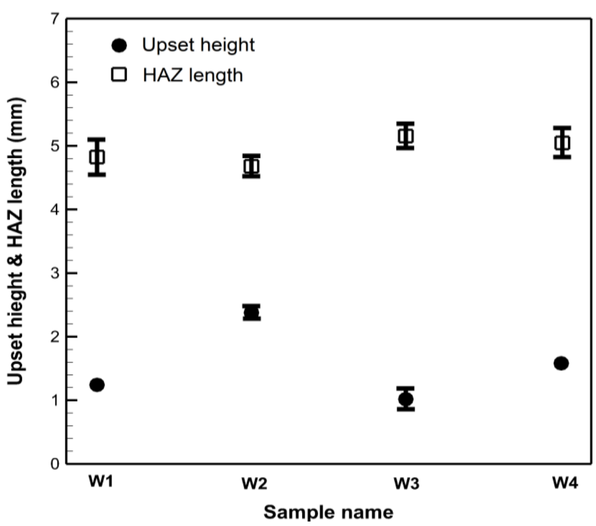

Fig. 3 Measured HAZ width and upset height in different welded samples.

It can be seen that higher welding current and upset pressure led to the formation of a more upset and narrower heat-affected zone for sample W2 in comparison to the W1 joint. A similar trend was almost observed for the W4 sample in comparison to the W3 joint. This is due to the fact that higher welding current generated more heat at the joint interface according to "Eq. 1". This increased the amount of melt and mushy metals formed in this region. On the other hand, higher upset pressure repelled this melt and mushy metal and led to the formation of higher upset and narrower heat-affected zone. Figure 4 shows the results of the tensile test performed on the base metal and welded samples produced by different welding conditions.

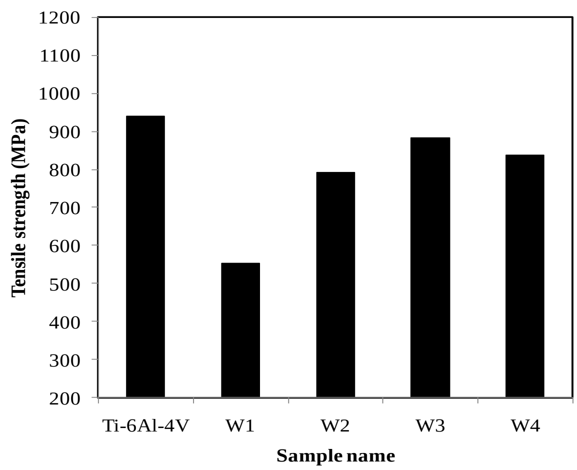

Fig. 4 Tensile test result of base material and welded samples.

In all samples, fracture occurred at the joint interface. It is observed that W1 joint welded with the highest welding current and the lowest upset pressure had the minimum tensile strength. An increase in the upset pressure improved tensile strength in the W2 joint but a decrease in the welding current had more effect on tensile strength of the joints in the case of W3 sample in such a way that it had the best tensile strength amongst all welds. In this condition, the tensile strength of the joint was about 94% of the base material. For the W4 sample, the strength of the joint decreased slightly with increasing the upset pressure.

In order to have a better understanding of the effects of upset welding parameters on the joint strength, microstructures of those welds which had the highest and the lowest tensile strengths were observed by optical and scanning electron microscopes. Figures 5(a) and (b) show low magnification SEM micrographs of the joint interface for W1 and W3 samples, respectively. For both of them, pores were formed during joining. However, by comparing these two macrographs, it is observed that the number and size of pores are considerably lower in the case of the W3 joint.

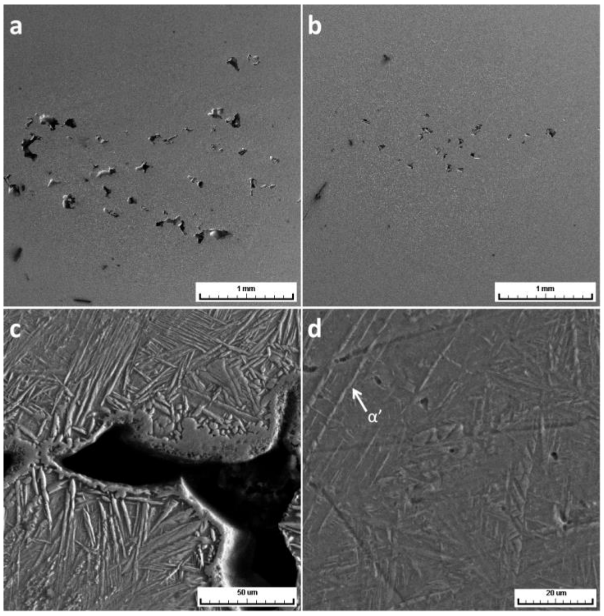

Fig. 5 SEM microstructures of the joint interface in: (a): W1 and (b): W3 samples. Higher magnification SEM micrographs of (c): pore and (d): joint interface

As stated by Kerstens and Richardson and Song [15], [18], the heat generated at the faying surfaces during welding was higher than that was produced by bulk resistance. As a consequence, the higher amount of heat developed more liquid metal at the interface. During upsetting, the liquid metal near the edges of the contact surfaces was rejected as flash and replaced with mushy metal, but the liquid metal at the center of the interface was trapped and solidified. Since the welding process was performed in ambient air and the cooling rate was too high, a large number of pores were formed in the molten metal as a result of trapping air gases including oxygen, hydrogen and nitrogen in the melt. However, by exerting higher upset pressure, more liquid metal was rejected from the interface which in turn decreased the pore volume fraction, considerably.

Similar results were reported by Sharifitabar et al. [13] during resistance upset welding of 304 austenitic stainless steel. Higher magnification SEM micrographs of pore and the joint interface are shown in “Figs. 5(c) and (d)”, respectively. It is evident that due to the high cooling rate of the joint interface after the welding process, non-equilibrium microstructure including ά martensite laths and Widmanstätten structure was formed at the joint interface [20].

Optical micrographs of the Ti-6Al-4V base plate in different magnifications are shown in “Figs. 6(a) and (b)”. The microstructure is bi-modal and contains α-β islands and equiaxed α grains. On the other hand, the weld zone microstructure in “Fig. 6(c) and (d)” contains ά martensite, α-β Widmanstätten laths and grain boundary α-phase which was formed at the primary β grain boundaries.

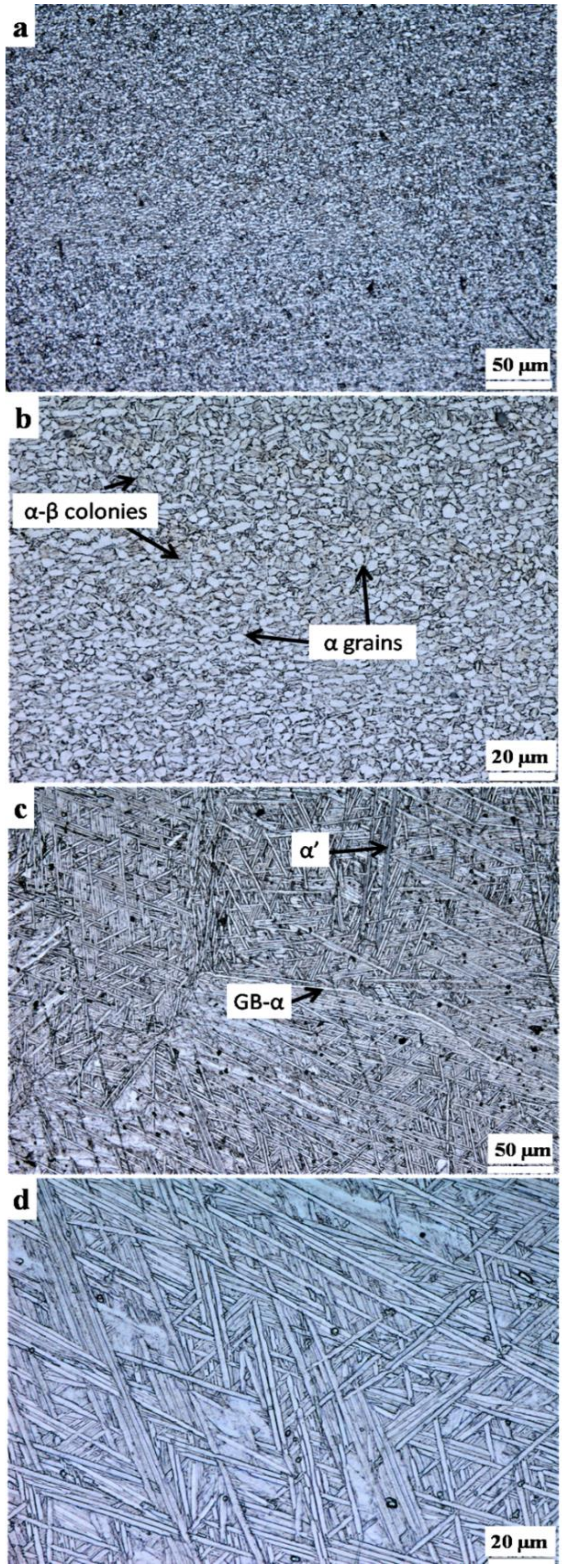

Fig. 6 Optical micrographs of Ti-6Al-4V alloy: (a), (b): parent metal, (c) and (d): weld zone.

It was previously stated that in Ti-6Al-4V alloy, martensite phase is formed under rapid solidification and cooling rate through a shear-type diffusionless transformation [19]. Furthermore, it is worth noting that both martensite and Widmanstätten microstructural features have detrimental effects on the elongation of the alloy [21].

In order to assess the effect of welding parameters on fracture mechanism, fracture surfaces of tensile test specimens were observed by SEM. Figures 7(a) and (b) show fracture surfaces of W1 and W3 specimens, respectively.

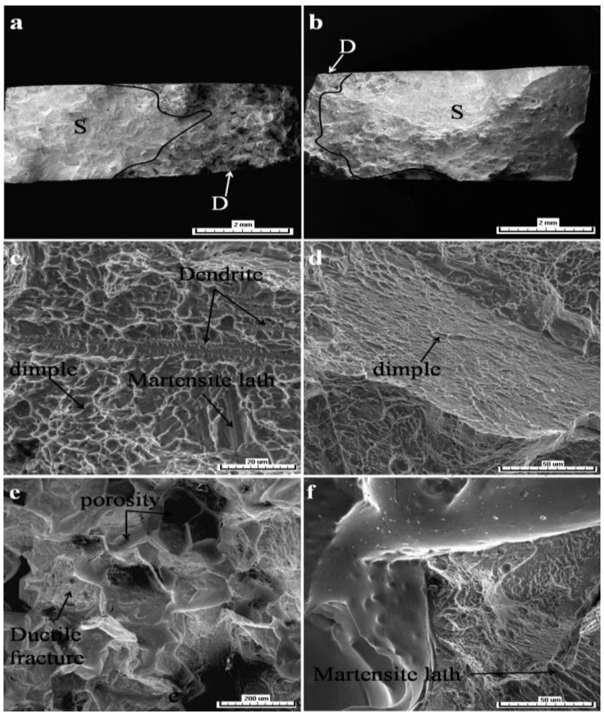

Fig. 7 SEM fracture surface features of :(a): W1 and (b): W3 samples, (c) and (d): are higher magnification of S region, respectively, (e) and (f): are higher magnification of D region.

Two different regions can be distinguished in these figures which are named by S (Retrieved from sound) and D (Retrieved from defective) letters on them. Also, these two regions are separated by a black line. The S/D area fraction is much higher in the W3 sample. Higher magnifications of the S region in W1 and W3 samples are shown in "Figs. 7(c) and (d)", respectively. The presence of dimples confirms the ductile fracture mode of the alloy in this region.

There are three long dendrite-like features in the fracture surface of the W1 sample which were formed as a result of melt solidification after the welding process. Furthermore, some lath-like features are detected which show the origination of cracks from the plate-like martensite phase. On the other hand, the D region has some voids with inter-granular fracture features as represented in "Fig. 7(e)". The fracture surface near a void is shown in "Fig. 7(f)". It is observed that the fracture mode is completely ductile with fine dimples. Moreover, the inner surface of the void is covered with a smooth thin adhesive layer which may be titanium oxide film.

It was previously stated that an increase in the welding current increased the amount of liquid metal formed at the joint interface in the W1 sample compared to the W3 joint. On the other hand, low welding pressure in sample W1 did not repel all the liquid metal from the interface. So, the dissolution of gases in the molten metal led to the formation of lots of pores during solidification. These pores had a detrimental effect on strength and therefore this sample had low tensile strength. The D region with a considerable surface area in "Fig. 7(a)" is representative of the solidified region containing porosity.

The application of higher welding pressure rejected more liquid metal from the interface. As a result, the S/D area fraction increased which improved the strength of the joint in the W3 sample.

The results of the micro-hardness test across half of the joint length for the W1 and W3 samples are presented in "Fig. 8".

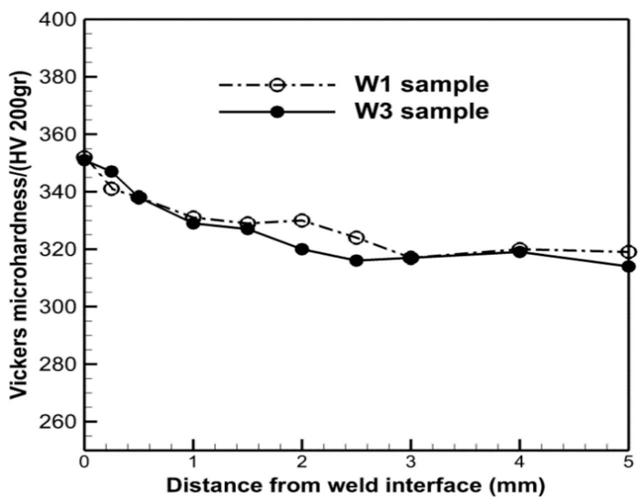

Fig. 8 Microhardness distribution graph across the weld interface in W1 and W3 joints.

The hardness variation trends in the two samples are almost the same. The joint interface has the highest hardness and it gradually decreased toward the base metal. Higher hardness in the joint interface most probably is due to the formation of martensite and Widmanstätten laths in this region, as well as the dissolution of atmospheric gases in the weld metal. It is generally accepted that in titanium alloys, the dissolution of oxygen in the weld metal increases hardness and deteriorates their ductility [2].

4 CONCLUSION

In the present study, microstructure and mechanical properties of resistance upset welded Ti-6Al-4V alloy were investigated. The obtained results can be summarized as follows.

1- Pores were formed at the joint interface in all samples and welding parameters including welding current and upset pressure had considerable influence on the volume fraction of pores. It was shown that melting and solidification was the main reason for the formation of pores.

2- Microstructural observations indicated the presence of martensite phase along with the Widmanstätten structure at the joint interface. As a consequence, the joint interface hardness had the highest value and it gradually decreased toward the base metal.

3- In the optimum condition, the tensile strength of the joint was up to 94% of the base metal. Fractography of the samples indicated that the presence of pores was the main reason for decreasing the joint strength.

5 REFERENCES

[1] Taylor, J. C., Hondrum, S. O., Prasad, A., and Brodersen, C. A., Effects of Joint Configuration For the Arc Welding of Cast Ti-6Al-4V Alloy Rods in Argon, The Journal of Prosthetic Dentistry Vol. 79, No. 3, 1998, pp. 291-297.

[2] Mathers, G., Welding of Titanium & Its Alloys, https://www.twi-global.com. 2019.

[3] Balasubramanian, V. V., Malarvizhi, S., Vijay, P., and Gourav, R. A., High Temperature Tensile Properties and Microstructural Characterization of Gas Tungsten Constricted Arc Welded Ti–6Al–4V Alloy, Materials Research Express, Vol. 6, No. 9, 2019, pp. 0965d6.

[4] Meshram, S. D., Mohandas, T., A Comparative Evaluation of Friction and Electron Beam Welds of Near-α Titanium Alloy, Materials & Design, Vol. 31, No. 4, 2010, pp. 2245-2252.

[5] Chiani, M., Atapour, M., A Study on the Stress Corrosion Cracking Susceptibility of Friction Stir Welded Ti-6Al-4V Alloy Joints, Materials Research Express, Vol. 6, No. 9, 2019, pp. 096598.

[6] Kahraman, N., Gülenç, B., and Findik, F., Joining of Titanium/Stainless Steel by Explosive Welding and Effect on Interface, Journal of Materials Processing Technology, Vol. 169, No. 2, 2005, pp. 127-133.

[7] Andreoli, A. F., Ponsoni, J. B., Soares, C., de Oliveira, M. F., and Kiminami, C. S., Resistance Upset Welding of Zr-Based Bulk Metallic Glasses, Journal of Materials Processing Technology, Vol. 255, 2018, pp. 760-764.

[8] Doyen, O., Gloannec, B. L., Deschamps, A., Geuser, F. D., Pouvreau, C., and Poulon-Quintin, A., Ferritic and Martensitic ODS Steel Resistance Upset Welding of Fuel Claddings: Weldability Assessment and Metallurgical Effects, Journal of Nuclear Materials, Vol. 518, 2019, pp. 326-333.

[9] Hamedi, M., Eisazadeh, H., and Esmailzadeh, M., Numerical Simulation of Tensile Strength of Upset Welded Joints with Experimental Verification, Materials & Design, Vol. 31, No. 5, 2010, pp. 2296-2304.

[10] Hasegawa, K., Resistance Butt Welding of Aluminium Alloys, Welding International Vol. 11, No. 3, 1997, pp. 206-211.

[11] Setty, D. S., Ravinder, R. P., and Murthy, A. L. N., Resistance Butt Welding of Zirconium Alloy Material, Materials and Manufacturing Processes, Vol. 23, No. 8, 2008, pp. 844-851.

[12] Sharifitabar, M., Halvaee, A., Resistance Upset Butt Welding of Austenitic to Martensitic Stainless Steels, Materials & Design, Vol. 31, No. 6, 2010, pp. 3044-3050.

[13] Sharifitabar, M., Halvaee, A., and S. Khorshahian, Microstructure and Mechanical Properties of Resistance Upset Butt Welded 304 Austenitic Stainless Steel Joints, Materials & Design, Vol. 32, No. 7, 2011, pp. 3854-3864.

[14] Min, K. B., Kim, K. S., and Kang, S. S., A Study on Resistance Welding in Steel Sheets Using a Tailor-Welded Blank (1st Report): Evaluation of Upset Weldability and Formability, Journal of Materials Processing Technology, Vol. 101, No. 1, 2000, pp. 186-192.

[15] Kerstens, N. F. H., Richardson, I. M., Heat Distribution in Resistance Upset Butt Welding, Journal of Materials Processing Technology, Vol. 209, No. 5, 2009, pp. 2715-2722.

[16] Le Gloannec, B., Doyen, O., Pouvreau, C., Doghri, A., and Poulon-Quintin, A., Numerical Simulation of Resistance Upset Welding in Rod to Tube Configuration with Contact Resistance Determination, Journal of Materials Processing Technology, Vol. 238, 2016, pp. 409-422.

[17] Ozlati, A., Movahedi, M., Effect of Welding Heat-Input on Tensile Strength and Fracture Location in Upset Resistance Weld of Martensitic Stainless Steel to Duplex Stainless Steel Rods, Journal of Manufacturing Processes, Vol. 35, 2018, pp. 517-525.

[18] Pradille, C., Bay, F., and Mocellin, K., An Experimental Study to Determine Electrical Contact Resistance, 2010 Proceedings of the 56th IEEE Holm Conference on Electrical Contacts, 2010, pp. 1-5.

[19] Kumar, K., Masanta, M., and Kumar Sahoo S., Microstructure Evolution and Metallurgical Characteristic of Bead-on-Plate TIG Welding of Ti-6Al-4V Alloy, Journal of Materials Processing Technology, Vol. 265, 2019, pp. 34-43.

[20] Xu, J., Zhu, J., Fan, J., Zhou, Q., Peng, Y., and Guo, S., Microstructure and Mechanical Properties of Ti–6Al–4V Alloy Fabricated Using Electron Beam Freeform Fabrication, Vacuum, Vol. 167, 2019, pp. 364-373.

[21] Christoph Leyens, M. P., Titanium and Titanium Alloys: Fundamentals and Applications, Wiley-VCH Verlag GmbH & Co. 2003.